*International Journal of Marine Engineering Innovation and Research, Vol. 11(2), Jun. 2026. 601-610*
*(pISSN: 2541-5972, eISSN: 2548-1479)*



# Numerical Analysis of Forward-Facing Reverse-V Step Hull Angle on Resistance Characteristics of Planing Hull

Amam Baharullah[1*], Sunarsih [2], Abdi Ismail [3]

(Received: 29 May 2026 / Revised: 30 May 2026 / Accepted: 4 June 2026 / Available Online: 8 June 2026)

***Abstract*****—** This study investigates the hydrodynamic resistance characteristics of a forward-facing reverse-V stepped planing hull using a Computational Fluid Dynamics (CFD) approach under high-speed planing conditions. Five reverse-V angle configurations consisting of 180°, 165°, 150°, 135°, and 120° were evaluated at a constant speed of 27 knots (13.9 m/s) using the Reynolds-Averaged Navier–Stokes (RANS) and Volume of Fluid (VOF) methods. Unlike conventional aft-facing stepped hulls, the proposed reverse-V geometry redirects the flow inward toward the forward centerline region beneath the hull bottom, modifying pressure redistribution, cavity interaction, and wetted surface formation. The numerical simulations employed a Poly-Hexacore meshing strategy and demonstrated stable convergence behavior with excellent mesh-quality characteristics. The results show that the 165° and 150° configurations increased hydrodynamic resistance due to stronger turbulence interaction and larger wetted surface development around the step region. In contrast, sharper reverse-V configurations improved hydrodynamic performance through stronger inward pressure convergence and more compact cavity formation. The 120° configuration generated the lowest resistance value of 7463.052 N and achieved the highest resistance reduction of 2.02% compared to the baseline model.

*Keywords*—Reverse-V Step Hull, Forward-Facing Step Hull, Double-Step Planing Hull, Hydrodinamic Resistance, Computational Fluid Dynamics (CFD)

**Coressponding Author: baharullahamam@gmail.com*

## I. INTRODUCTION

High-speed marine transportation continues to develop rapidly due to increasing operational demands for fast, efficient, and fuel-saving vessels in patrol, rescue, military, and recreational applications [1]. *Planing hull* vessels are widely utilized in high-speed craft because hydrodynamic lift generated at high operational speeds enables the hull to partially rise above the free surface, thereby reducing hull immersion and improving speed performance [1], [2]. Hydrodynamic lift generated during planing conditions significantly influences *wetted surface area*, running trim, sinkage, and resistance characteristics [2].

Resistance remains one of the primary hydrodynamic problems in *high-speed planing hulls* because increasing vessel speed directly increases propulsion power requirements and fuel consumption [3]. Total resistance in planing vessels generally consists of *frictional resistance* and *pressure resistance* generated by fluid interaction beneath the hull bottom [4]. Frictional resistance strongly depends on *wetted surface area*, while pressure drag is influenced by local pressure distribution and flow behavior around the hull surface [3], [4]. Excessive wetted surface area therefore increases wall shear stress and contributes to higher hydrodynamic resistance characteristics [1].

Savitsky established the fundamental hydrodynamic theory of *planing hulls* by demonstrating that lift generation beneath the hull bottom strongly affects resistance characteristics and dynamic running attitude [1]. Taunton et al. further demonstrated that pressure distribution beneath hard-chine planing hulls significantly influences running trim, wetted length, and calm-water resistance characteristics [2]. Faltinsen also emphasized that flow separation, pressure drag, and hydrodynamic instability become dominant parameters in high-speed marine vehicles operating under planing conditions [3]. Lewis explained that viscous resistance and pressure resistance are strongly governed by hull geometry and free-surface interaction beneath the hull bottom [4].

CFD-based hydrodynamic analysis has become increasingly important in modern planing hull investigations because numerical methods enable detailed visualization of pressure distribution, cavity formation, wetted surface development, and free-surface flow behavior [5]. Mancini et al. proposed CFD guidelines for planing hull simulations and demonstrated that accurate free-surface resolution significantly affects resistance prediction capability [5]. Hosseini et al. compared several CFD turbulence models and confirmed that numerical approaches provide reliable prediction accuracy for planing hull resistance analysis [6]. Judge et al. also validated CFD prediction capability for deep-V planing hulls through experimental comparison under

Amam Baharullah is with Departement of Marine Engineering, Insti tut Teknologi Sepuluh Nopember, Surabaya, 60111, Indonesia. E-mail: baharullahamam@gmail.com
Sunarsih is with Departement of Marine Engineering, Insti tut Teknologi Sepuluh Nopember, Surabaya, 60111, Indonesia. E-mail : sunarsih@gmail.com
Abdi Ismail is with the Research Center for Hydrodynamic Technology, National Research and Innovation Agency (BRIN), Surabaya 60117, Indonesia. E-mail: abdi004@brin.go.id

calm-water conditions [7]. Recent hydrodynamic reviews consequently confirmed that resistance optimization remains one of the major research challenges in modern high-speed craft development [8].

The implementation of *stepped hull* geometry has become one of the most widely applied approaches for reducing resistance in *planing hull* vessels [9]. Conventional stepped hulls generally employ *aft-facing V-step* geometries to promote downstream ventilation and flow separation beneath the hull bottom [9]. Flow separation occurring behind the step region generates a *ventilated cavity* that reduces wetted surface area and decreases frictional resistance [10]. Lower wetted surface area subsequently improves hydrodynamic efficiency and reduces total resistance characteristics [10].

Rayhan et al. investigated the influence of *step angle variation* on resistance characteristics of stepped planing hulls using CFD methods [9]. Their investigation demonstrated that larger step angles generated lower resistance characteristics, where the 270° configuration produced the lowest resistance among the investigated models [9]. Sulman et al. numerically investigated *single-step* and *double-step* hull configurations using *Reynolds-Averaged Navier-Stokes* (RANS) and *Volume of Fluid* (VOF) methods [10]. Their investigation demonstrated that cavity formation and wetted surface reduction significantly affect dynamic trim, sinkage, and resistance characteristics [10].

Trimulyono et al. analyzed the influence of *double-step position* on *planing hull* hydrodynamic performance using *unsteady Reynolds-Averaged Navier-Stokes* (uRANS) simulations combined with overset mesh techniques [11]. Their investigation demonstrated that step position affects pressure redistribution beneath the hull bottom and influences total resistance characteristics [11]. Bilandi et al. demonstrated that CFD approaches provide reliable prediction capability for analyzing wetted surface characteristics, ventilation behavior, and resistance performance in stepped planing hulls [12]. Bilandi et al. also confirmed that cavity formation significantly influences hydrodynamic stability and resistance characteristics in *double-stepped planing hulls* [13].

Several recent investigations further analyzed the influence of geometric modifications on hydrodynamic resistance mechanisms in stepped planing hulls [14]. Tavakoli et al. demonstrated that cavity formation strongly affects pressure redistribution beneath the hull bottom in *double-stepped planing hulls* [14]. Dashtimanesh et al. confirmed that step geometry significantly influences wetted surface characteristics during planing operation [15]. Lakatoš et al. demonstrated that local geometric modifications alter pressure distribution and influence lift generation mechanisms in high-speed craft [16]. Zou et al. investigated geometric modifications beneath *double-stepped planing hulls* and demonstrated that hydrodynamic performance strongly depends on local pressure-field development [17]. Hidayat et al. also confirmed that bottom-surface modifications significantly affect resistance characteristics under full-planing conditions [18].

Recent investigations additionally focused on hydrodynamic modeling and resistance prediction of high-speed planing hulls [19]. Tavakoli et al. proposed hydrodynamic modeling approaches for planing boats and demonstrated that local flow instability strongly affects resistance characteristics [19]. Roshan et al. confirmed that pressure redistribution beneath the hull significantly influences hydrodynamic efficiency in high-speed craft [20]. Tavakoli et al. also demonstrated that stepped hull geometry significantly affects cavity stability and calm-water hydrodynamic performance [21]. Sulman et al. further investigated pressure distribution and ventilation characteristics in *multi-step planing hulls* and demonstrated that cavity development strongly influences resistance mechanisms [22]. Matveev numerically investigated various stepped hull configurations and demonstrated that swept-step geometries significantly influence cavity behavior and hydrodynamic lift generation beneath the hull bottom [23].

Existing stepped hull investigations predominantly employ conventional *aft-facing V-step* geometries to induce downstream ventilation and reduce wetted surface area through cavity formation mechanisms [23]. Previous studies mainly focused on *step angle variation*, *step height*, *step position*, *step spacing*, and *multi-step configurations* under conventional aft-facing hydrodynamic arrangements [22]. Existing literature therefore remains limited to conventional downstream flow-separation mechanisms.

However, limited studies investigate *forward-facing reverse-V step geometries* and their influence on pressure redistribution, cavity formation, wetted surface development, and resistance characteristics [24]. Hydrodynamic mechanisms generated by reverse-facing step configurations remain unclear because reverse geometries potentially alter cavity behavior, local pressure fields, lift generation, and flow reattachment patterns beneath the hull bottom [23], [24]. Existing studies discussing reverse-facing step geometries only introduced general geometric concepts without providing detailed hydrodynamic resistance analysis for *forward-facing reverse-V step angle variations* in *double-step planing hulls* [24].

No previous investigation specifically analyzes the influence of *forward-facing reverse-V step angles* on resistance characteristics using CFD methods under multiple reverse-angle configurations. Existing stepped hull investigations therefore remain limited to conventional aft-facing hydrodynamic mechanisms and have not comprehensively examined reverse-facing cavity behavior, reverse-step pressure redistribution, and reverse-V resistance mechanisms. These conditions indicate that the present investigation introduces a new hydrodynamic stepped-hull configuration that has not been comprehensively analyzed in previous CFD-based stepped planing hull studies.

The present study investigates the influence of *forward-facing reverse-V step angles* on the resistance characteristics of a *double-step planing hull* using a CFD approach. Five reverse-V angle configurations consisting of 180°, 165°, 150°, 135°, and 120° are analyzed to evaluate their effects on pressure distribution, cavity formation, wetted surface area, and total resistance characteristics. The present investigation aims to identify the hydrodynamic behavior of reverse-facing stepped configurations and provide a new resistance-reduction approach for high-speed planing hull applications.

## II. METHOD

The present study investigates the hydrodynamic characteristics of a forward-facing reverse-V stepped planing hull using the Computational Fluid Dynamics (CFD) method. The parent hull geometry employed in this investigation is an FRP patrol boat categorized as a Special Service Ship operating under high-speed planing conditions. The hull represents a hard-chine deep-V planing hull commonly utilized in patrol and rapid-response marine operations. According to Savitsky [1], hydrodynamic lift generation and wetted surface area significantly influence the resistance characteristics of planing hulls. Taunton et al. [2] additionally demonstrated that pressure distribution beneath the hull bottom strongly affects calm-water resistance performance. The principal dimensions of the parent hull are summarized in Table 1.

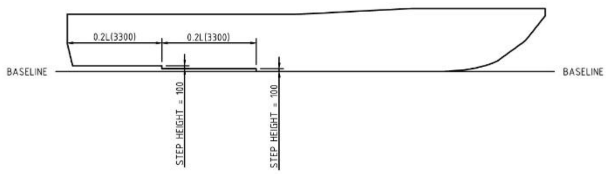


**Figure 1. Ship with step hull**

TABLE 1.
SHIP SPECIFICATIONS

| Ship Specifications | | | |
|---|---|---|---|
| Length Overall | LOA | 16.70 | m |
| Length Waterline | LWL | 16.50 | m |
| Beam | B | 3.80 | m |
| Hull Beam | H | 3.90 | m |
| Maximum Height | Hmax | 4.40 | m |
| Design Draft | T | 0.70 | m |
| Speed Operational | Vs | 22.00 | knots |
| Maximum Speed | Vmax | 27.00 | knots |
| Deadrise Angle | β | 20° | |
| Hull Type | - | Planing Hull | |
| Material | - | FRP | |
| Main Engine | | 3 x 300 | HP |

According to Faltinsen [3], high-speed craft operating at high Froude-number conditions generate significant hydrodynamic lift beneath the hull bottom, resulting in wetted surface reduction during planing operation. The Froude number is expressed as follows:

$$Fn = \frac{V}{\sqrt{g.L}} \quad (1)$$

where *Fn* is the Froude number, *V* is ship velocity (m/s), *g* is gravitational acceleration (m/s²), and *L* is ship length (m).

Conventional stepped hull configurations generally employ *aft-facing V-step* geometries to induce downstream ventilation and cavity formation beneath the hull bottom [9], [10]. Flow separation occurring behind the step region subsequently reduces wetted surface area and frictional resistance [10], [12]. However, existing investigations predominantly focus on aft-facing step geometries, while investigations concerning *forward-facing reverse-V configurations* remain extremely limited.

The present investigation introduces a *forward-facing reverse-V step geometry* intended to modify the hydrodynamic mechanism beneath the hull bottom. Unlike conventional aft-facing steps, the reverse-V arrangement redirects the flow toward the centerline region and potentially induces *pressure convergence* beneath the hull surface. This mechanism is expected to alter cavity development, wetted surface redistribution, and local flow reattachment characteristics.

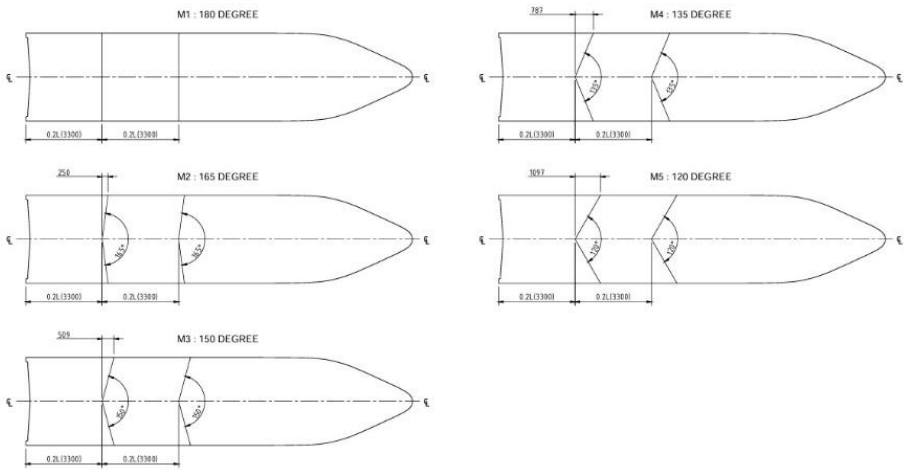


**Figure 2.** Reverse-V Step Configuration (120°, 135°, 150°, 165°, 180°)

The reverse-facing geometry potentially modifies local pressure distribution by generating inward flow redirection beneath the hull bottom. Conventional aft-facing steps generally release pressure toward downstream regions, whereas the reverse-V arrangement may produce localized pressure concentration toward the centerline region. This mechanism is expected to influence cavity topology and wetted area redistribution beneath the hull.

Five reverse-V angle configurations of 180°, 165°, 150°, 135°, and 120° were investigated in the present study. The 180° configuration represents a straight step geometry without inward flow convergence effects beneath the hull bottom. Meanwhile, the 165° and 150° configurations introduce moderate inward flow redirection toward the centerline region, leading to gradual pressure convergence beneath the hull surface. More aggressive configurations, namely 135° and 120°, generate stronger inward flow interaction and more concentrated local pressure development beneath the hull bottom. As the reverse-V angle decreases, the cavity redistribution mechanism is expected to become more pronounced, potentially affecting wetted surface development and local flow reattachment characteristics more significantly [9], [10].

The forward-facing reverse-V step configurations investigated in this study are illustrated in Figure 2. As shown in Figure 2, the reverse-V angles were applied at the step region to examine their influence on pressure distribution, cavity formation, wetted surface area, and the overall hydrodynamic resistance characteristics of the planing hull.

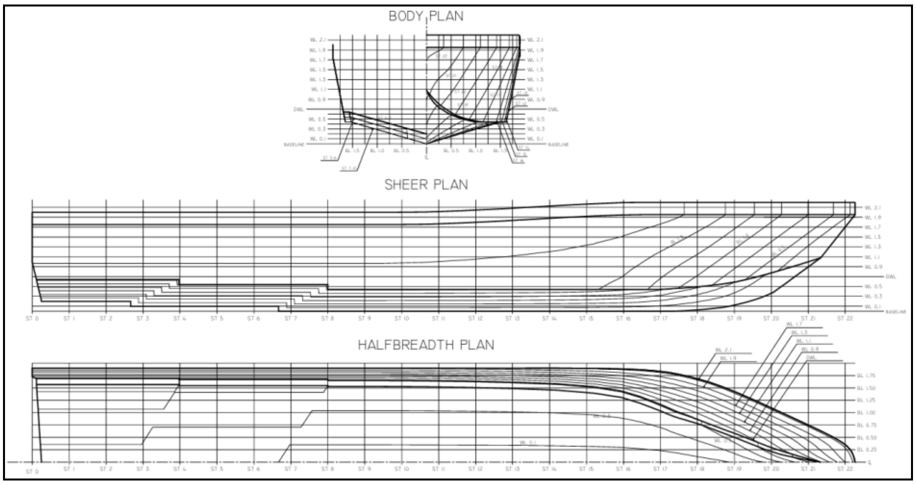


**Figure 3.** Linesplan Existing (M1 : 180°)

The longitudinal spacing between successive steps was fixed at 0.20L for all modified configurations. Previous investigations demonstrated that longitudinal spacing within the range of 0.15L–0.25L generally produces stable cavity development and favorable hydrodynamic performance [10], [11]. Sulman et al. [10] and Trimulyono et al. [11] demonstrated that excessively small spacing weakens cavity stability, whereas excessively large spacing reduces hydrodynamic interaction between successive steps. The spacing parameter was therefore intentionally fixed at 0.20L to isolate the hydrodynamic influence of reverse-V geometry and eliminate interference caused by spacing variation.

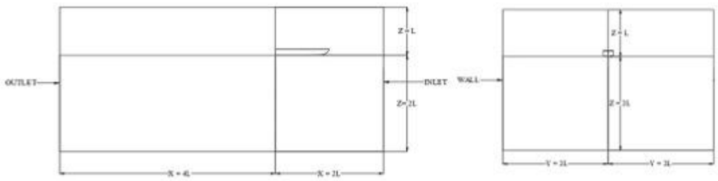

**Figure 4.** Boundary condition baset on hull length

The present study evaluates four hull configurations consisting of one baseline model and three modified reverse-V models. The baseline model represents the conventional aft-facing stepped hull, while the modified models employ forward-facing reverse-V arrangements under double-step and triple-step configurations. All simulations were conducted at a constant operating speed of 27 knots (~13.9 m/s) under planing conditions to evaluate the influence of reverse-V geometry on hydrodynamic resistance characteristics.

TABLE 2.
MADEL VARIATION

| Model | Type | Angle | Spacing | Speed (m/s) |
|---|---|---|---|---|
| M1 | Double Step Hull | 180° | 0.2L | 13.9 |
| M2 | Double Reverese-V (<) | 165° | 0.2L | 13.9 |
| M3 | Double Reverese-V (<) | 150° | 0.2L | 13.9 |
| M4 | Double Reverese-V (<) | 135° | 0.2L | 13.9 |
| M5 | Double Reverese-V (<) | 120° | 0.2L | 13.9 |

According to Lewis [4], total ship resistance is strongly influenced by hull geometry, velocity, wetted surface area, and fluid characteristics. The total resistance equation is expressed as follows:

$$RT = \frac{1}{2}\rho . S . V^2 \tag{2}$$

where $RT$ is total resistance (N), $\rho$ is fluid density (kg/m³), $S$ is wetted surface area (m²), and $V$ is ship velocity (m/s).

The Reynolds number was additionally utilized to determine the flow regime surrounding the hull geometry. The Reynolds number is expressed as follows:

$$Re = \frac{V.L}{\vartheta} \tag{3}$$

where $Re$ is Reynolds number, $V$ is ship velocity (m/s), $L$ is hull length (m), and $\vartheta$ is kinematic viscosity (m²/s).

The CFD simulation process consisted of geometry generation, meshing, numerical setup, and simulation stages. The numerical simulations were conducted using the *Reynolds-Averaged Navier–Stokes* (*RANS*) approach under steady-state conditions. According to Mancini et al. [5], the RANS approach provides reliable prediction capability for pressure distribution and resistance characteristics in high-speed planing hull simulations. The governing equation for incompressible turbulent flow is expressed as follows:

$$\rho \bar{u}_j \frac{\delta \bar{u}_j}{\delta x_j} = \rho \bar{f}_i + \frac{\delta}{\delta x_j}\left[-\bar{p}\delta_{ij} + \mu\left(\frac{\delta \bar{u}_i}{\delta x_j} + \frac{\delta \bar{u}_j}{\delta x_i}\right) - \overline{\rho u'_i u'_j}\right] \tag{4}$$

The free-surface flow was modeled using the *Volume of Fluid* (*VOF*) method to capture the air-water interface surrounding the hull geometry. The *k-ω SST* turbulence model was employed because it provides reliable prediction capability for flow separation, pressure redistribution, and cavity formation mechanisms in stepped planing hull simulations [5], [6], [10].

The computational domain and boundary conditions were generated according to ITTC recommendations for high-speed craft CFD simulations [25], [26]. The inlet boundary was positioned at a distance of 2L ahead of the hull, while the outlet boundary was placed 4L behind the hull. The side boundary was positioned at 2L from the hull centerline, and the top boundary was located at 1L above the free surface. Velocity inlet conditions were applied at the upstream boundary, while pressure outlet conditions were imposed at the downstream boundary. Symmetry conditions were additionally applied along the center plane to reduce computational cost.

The numerical convergence was evaluated based on residual reduction and stabilization of resistance values during the iterative solution process. The simulation was considered converged when the residual values reached asymptotic behavior and the resistance coefficient no longer exhibited significant fluctuation. The mean percentage error was calculated using the following equation:

$$M\,D = \frac{1}{N}\sum_{1}^{N}\left(\frac{dpre-dexp}{dexp}\right)100 \qquad (5)$$

where *MD* is the mean deviation (%), *dpre* is predicted data, *dexp* is experimental/reference data, and *N* is the total number of observed data.

## III. Results and Discussion

The numerical simulation was conducted to investigate the hydrodynamic characteristics of the *forward-facing reverse-V stepped planing hull* under high-speed planing conditions. The investigation focuses on the influence of reverse-V geometry on resistance characteristics, wetted surface redistribution, pressure convergence behavior, cavity interaction, and flow structure modification beneath the hull bottom. The discussion structure follows the numerical investigation framework presented in *Numerical Study on Resistance of Stepped Planing Hull* [9], while emphasizing the hydrodynamic mechanism associated with *reverse pressure redistribution* generated by the forward-facing reverse-V geometry.

The numerical stability and mesh independence were first evaluated before analyzing the hydrodynamic performance of each configuration. The mesh refinement procedure employed unstructured tetrahedral elements combined with prism-layer inflation near the hull surface to accurately capture free-surface interaction, pressure gradients, and cavity development beneath the hull bottom. Fine mesh concentration was applied around the reverse-V step region because the area experiences strong pressure redistribution and local flow separation.

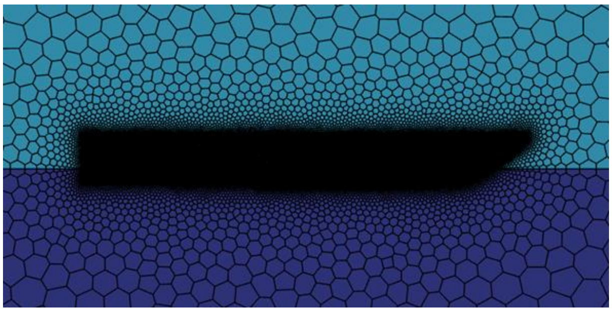

**Figure 5.** Meshing

In addition, the computational domain employed the Poly-Hexacore meshing method to improve numerical efficiency and flow-resolution capability during the CFD simulation process. The method combines polyhedral cells near the hull surface with hexahedral core refinement in the outer domain, providing better mesh quality, improved convergence stability, and lower computational cost compared to conventional tetrahedral meshes. Local mesh refinement was applied around the reverse-V step region to accurately capture pressure redistribution, flow separation, cavity formation, and free-surface interaction beneath the hull bottom. The meshing configuration used in the present study is illustrated in Figure 5.

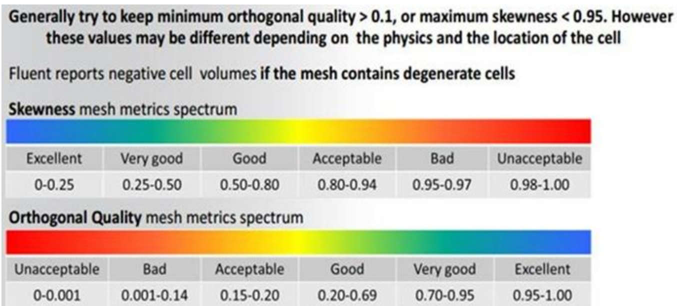


**Figure 6.** Skewness and orthogonal quality mesh metrics spectrums [27].

TABLE 3.
CONVERGENCE BASED ON SKEWNESS MESH METRIC SPECTRUM

| Model | Average Sqewness | Category |
|---|---|---|
| M1 | 0.011004624 | Excellent |
| M2 | 0.0099999079 | Excellent |
| M3 | 0.010395131 | Excellent |
| M4 | 0.010538279 | Excellent |
| M5 | 0.010393925 | Excellent |

Convergence testing is performed to ensure the accuracy of the finite element model by determining the optimal element size in the mesh. Stress results are compared across different mesh variations until the results stabilize. Mesh metric values are used to assess the convergence of the model, ensuring the reliability of the analysis results in Figure 6 [27].

Convergence testing was performed to ensure mesh accuracy and numerical stability. Based on Table 3, all mesh configurations achieved excellent mesh quality, with average skewness values ranging from 0.009999 to 0.010539. These results indicate that the computational mesh has reached satisfactory convergence and is suitable for reliable CFD analysis.

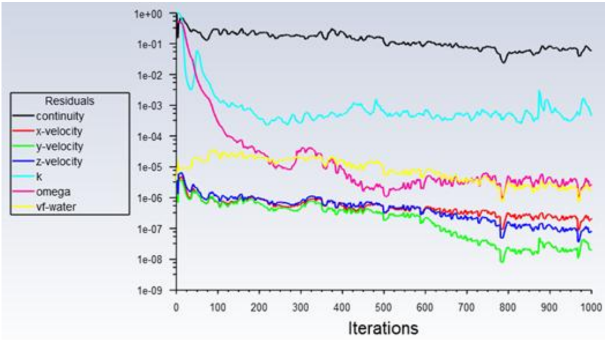


**Figure 7.** Residual Convergence History

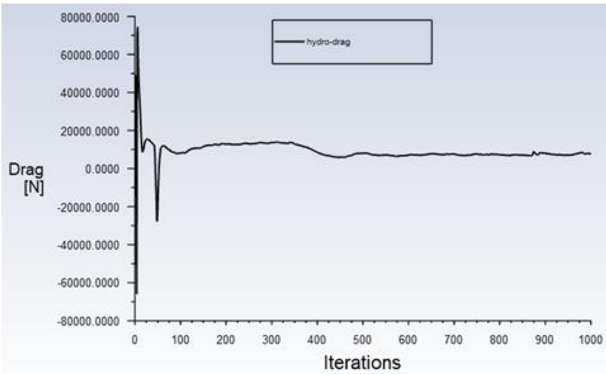


**Figure 8.** Force Convergence History

Figure 7 and 8 demonstrates stable convergence behavior for all numerical simulations. The residual values gradually decreased and approached asymptotic conditions as the iterative process progressed. The velocity residuals decreased to the order of $10^{-6}$-$10^{-7}$ while turbulence and volume-fraction residuals stabilized around $10^{-4}$-$10^{-5}$. In addition, the hydrodynamic force history exhibited stable behavior without significant fluctuation after several iterations, indicating that the numerical solution achieved satisfactory convergence. These stable convergence characteristics indicate that the numerical setup and mesh refinement strategy provide sufficient accuracy for predicting the hydrodynamic resistance characteristics of the reverse-V stepped hull configurations. Similar convergence behavior was also reported in stepped-hull CFD investigations conducted [5], [10].

TABLE 3.
RESISTANCE REDUCTION OF REVERSE-V STEPPED HULL

| Model | Resistance (N) | Reduction (%) |
|---|---|---|
| M1 | 7617.264 | 0 |
| M2 | 7787.926 | +2.24 |
| M3 | 8216.492 | +7.87 |
| M4 | 7490.366 | -1.67 |
| M5 | 7463.052 | +2.02 |

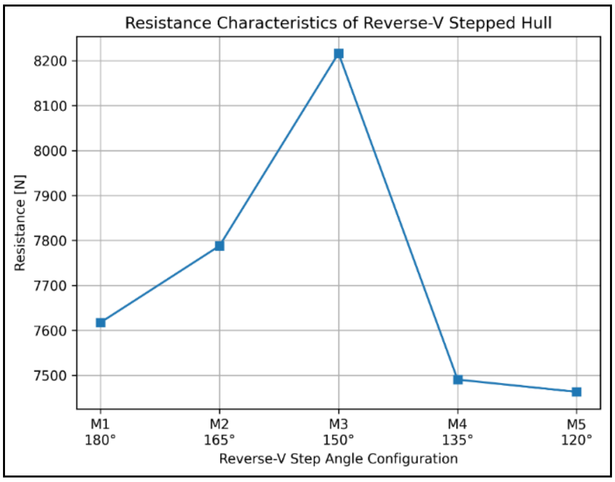


**Figure 9.** Resistance vs Variation Configuration

Figure 9 and Table 3 present the hydrodynamic resistance characteristics of all reverse-V stepped hull configurations. The results show that the reverse-V geometry significantly affected resistance behavior through modifications in pressure redistribution, cavity interaction, and wetted surface formation beneath the hull bottom. Unlike conventional aft-facing stepped hulls, the forward-facing reverse-V geometry redirected the flow inward toward the centerline region, altering the hydrodynamic mechanism beneath the hull.

The M2 (165°) and M3 (150°) configurations increased resistance by 2.24% and 7.87%, respectively, compared to the baseline model M1. These moderate reverse-V angles intensified local turbulence and pressure interaction around the step region, leading to larger wetted surface development and higher hydrodynamic drag.

In contrast, the sharper reverse-V configurations improved hydrodynamic performance. The M4 (135°) configuration reduced resistance by 1.67%, while the M5 (120°) configuration produced the lowest resistance value of 7463.052 N with the highest resistance reduction of 2.02%. The stronger inward pressure convergence generated by the sharper reverse-V geometry reduced wetted surface formation more effectively and improved cavity interaction stability beneath the hull bottom.


**(10.a)**


**(10.b).**

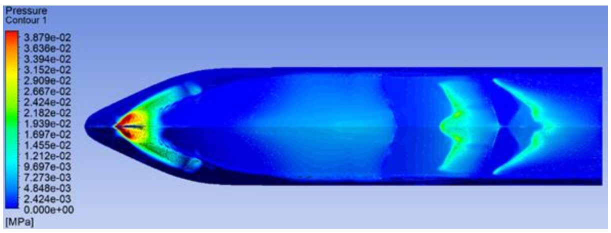


**(10.c).**

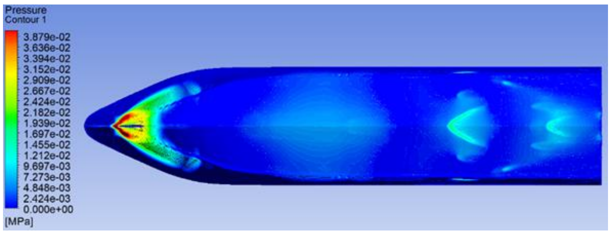


**(10.d).**

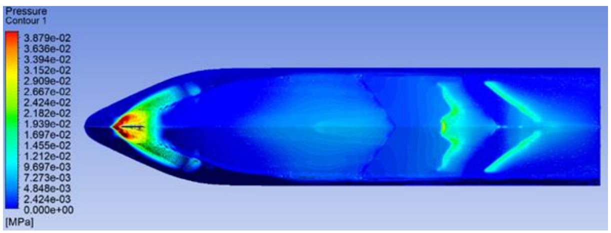


**(10.e).**

**Figure 10.** Bottom pressure distribution of reverse-V stepped hull (a) M1-180°, (b) M2-165°, (c) M3-150°, (c) M3-150Â°, (d) M4-135°, (e) M5-120°

Figure 10 shows that the reverse-V geometry significantly affected the pressure distribution beneath the hull bottom. The baseline model M1 (180°) produced a relatively elongated pressure field along the longitudinal direction. Meanwhile, the M2 (165°) and M3 (150°) configurations generated wider pressure interaction around the step region, increasing turbulence intensity and wetted surface formation.

In contrast, the sharper reverse-V configurations M4 (135°) and M5 (120°) produced more concentrated pressure convergence toward the centerline region. The M5 configuration generated the most compact pressure distribution and strongest cavity contraction, resulting in reduced wetted surface development and the lowest resistance among all investigated models

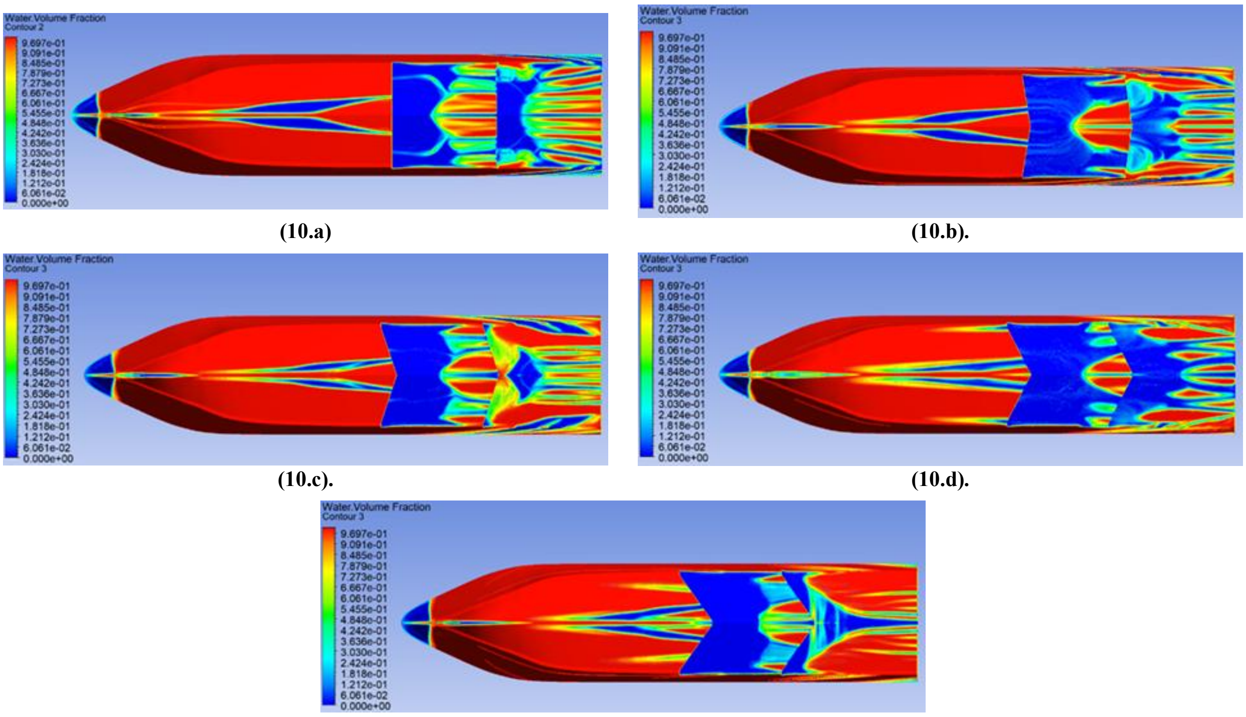


(10.a) (10.b). (10.c). (10.d). (10.e).

**Figure 11.** Velocity Volume Fraction contour of reverse-V stepped hull (a) M1-180°, (b) M2-165°, (c) M3-150°, (c) M3-150Â°, (d) M4-135°, (e) M5-120°

Figure 11 presents the water volume fraction and velocity contour of all reverse-V stepped hull configurations. The results show that the reverse-V geometry significantly influenced cavity development and flow structure beneath the hull bottom. The baseline model M1 (180°) produced a relatively elongated downstream cavity with wider flow dispersion behind the step region.

The M2 (165°) and M3 (150°) configurations generated stronger flow interaction around the reverse-V step, resulting in more irregular cavity structures and wider turbulent flow regions beneath the hull. These conditions increased local flow instability and contributed to larger wetted surface development.

In contrast, the sharper reverse-V configurations M4 (135°) and M5 (120°) produced more concentrated inward flow toward the centerline region. The M5 configuration generated the most compact cavity structure and smoother downstream flow pattern, indicating stronger cavity contraction and more stable flow redistribution beneath the hull bottom. These characteristics contributed to improved hydrodynamic performance and lower resistance values.

## IV. Conclusion

This study investigated the hydrodynamic resistance characteristics of a forward-facing reverse-V stepped planing hull using the CFD method under high-speed planing conditions. The results demonstrate that the reverse-V geometry significantly influences pressure redistribution, cavity interaction, wetted surface development, and total resistance beneath the hull bottom.

The moderate reverse-V configurations, namely M2 (165°) and M3 (150°), produced higher resistance values due to stronger turbulence generation and wider wetted surface development around the step region. In contrast, the sharper reverse-V configurations, namely M4 (135°) and M5 (120°), demonstrated improved hydrodynamic performance through stronger inward pressure convergence and more compact cavity formation beneath the hull bottom.

Among all investigated configurations, the M5 (120°) model generated the lowest resistance value of 7463.052 N and achieved the highest resistance reduction of 2.02% compared to the baseline model. The sharper reverse-V geometry produced more stable cavity interaction and reduced wetted surface area more effectively, resulting in lower hydrodynamic drag during planing operation.

Overall, the present investigation confirms that the reverse-V step angle is an important parameter affecting the hydrodynamic performance of stepped planing hulls. Smaller reverse-V angles tend to improve resistance-reduction performance by enhancing inward flow convergence and cavity redistribution beneath the hull surface.

## ACKNOWLEDGEMENTS

The author would like to thank all individuals and institutions who indirectly supported this research through access to data, facilities, and academic feedback.

## REFERENCES

[1] D. Savitsky, "Hydrodynamic design of planing hulls," Marine Technology, vol. 1, no. 1, pp. 71–95, Oct. 1964.

[2] D. J. Taunton, D. Hudson, and R. Shenoi, "Characteristics of a series of high-speed hard chine planing hulls—Part 1: Performance in calm water," International Journal of Small Craft Technology, vol. 122, no. A1, pp. 1–12, 2010.

[3] O. M. Faltinsen, Hydrodynamics of High-Speed Marine Vehicles. Cambridge, U.K.: Cambridge Univ. Press, 2005, pp. 125–241.

[4] E. V. Lewis, Principles of Naval Architecture Series: Resistance, Propulsion and Vibration. Jersey City, NJ, USA: SNAME, 2015, pp. 45–118.

[5] S. Mancini, F. De Luca, and A. Pensa, "Towards CFD guidelines for planing hull simulations based on the Naples systematic series," Journal of Marine Science and Engineering, vol. 9, no. 3, pp. 1–17, Mar. 2021.

[6] A. Hosseini, S. Tavakoli, A. Dashtimanesh, P. K. Sahoo, and M. Kõrgesaar, "Performance prediction of a hard-chine planing hull by employing different CFD models," Journal of Marine Science and Engineering, vol. 9, no. 5, pp. 1–21, May 2021.

[7] C. Judge, D. Troesch, and M. Perlin, "Experiments and CFD of a high-speed deep-V planing hull—Part I: Calm water," Applied Ocean Research, vol. 90, pp. 1–14, Sep. 2019.

[8] S. Tavakoli et al., "A review on the hydrodynamics of planing hulls," Ocean Engineering, vol. 302, pp. 1–28, 2024.

[9] F. A. Rayhan, A. Masrul, A. K. Akbar, and B. A. Putra, "Numerical study on resistance of stepped planing hull," Journal of Mechanical Engineering Science and Technology, vol. 7, no. 2, pp. 106–118, Aug. 2023.

[10] M. Sulman, S. Mancini, and R. N. Bilandi, "Numerical investigation of single and double steps in planing hulls," Journal of Marine Science and Engineering, vol. 12, no. 4, pp. 1–26, Apr. 2024.

[11] A. Trimulyono, M. L. Hakim, C. Ardhan, S. T. P. Ahmad, T. Tuswan, and A. W. B. Santosa, "Analysis of the double steps position effect on planing hull performances," Brodogradnja, vol. 74, no. 4, pp. 41–72, Dec. 2023.

[12] R. N. Bilandi, S. Tavakoli, S. Mancini, and A. Dashtimanesh, "Comparative study of experimental and CFD results for stepped planing hulls," Ocean Engineering, vol. 280, pp. 1–15, Jul. 2023.

[13] R. N. Bilandi, S. Tavakoli, and A. Dashtimanesh, "Seakeeping of double-stepped planing hulls," Ocean Engineering, vol. 236, pp. 1–14, Oct. 2021.

[14] S. Tavakoli, A. Dashtimanesh, and R. N. Bilandi, "Hydrodynamic study of heeled double-stepped planing hulls using CFD and 2D+T method," Ocean Engineering, vol. 196, pp. 1–17, Feb. 2020.

[15] A. Dashtimanesh, R. Khosravani, and S. Tavakoli, "Numerical study on a heeled one-stepped boat moving forward in planing regime," Applied Ocean Research, vol. 96, pp. 1–12, Jan. 2020.

[16] M. Lakatoš, T. Sahk, H. Andreasson, and K. Tabri, "The effect of spray rails, chine strips and V-shaped spray interceptors on the performance of low planing high-speed craft in calm water," Applied Ocean Research, vol. 122, pp. 1–17, May 2022.

[17] J. Zou, Y. Wang, X. Li, and H. Zhang, "Experimental and numerical research on the influence of stern flap mounting angle on double-stepped planing hull hydrodynamic performance," Journal of Marine Science and Engineering, vol. 12, no. 6, pp. 1–22, Jun. 2024.

[18] I. N. Hidayat, A. Prabowo, and S. Nugroho, "Analysis of stern flap application on planing hulls to reduce resistance using CFD," Mekanika, vol. 24, no. 2, pp. 87–96, 2025.

[19] S. Tavakoli, A. Dashtimanesh, and P. K. Sahoo, "An oblique 2D1T approach for hydrodynamic modeling of yawed planing boats in calm water," Journal of Ship Production and Design, vol. 38, no. 2, pp. 145–158, 2018.

[20] M. Chillemi, F. Cucinotta, and F. Sfravara, "Hydrodynamic analysis of a stepped planing hull through sea trials and CFD simulations," Technology and Science for the Ships of the Future, pp. 1–15, 2025.

[21] F. Pacuraru, A. Mandru, and A. Bekhit, "CFD study on hydrodynamic performances of a planing hull," Journal of Marine Science and Engineering, vol. 10, no. 10, p. 1523, 2022.

[22] S. Park, Z. Wang, F. Stern, N. Husser, S. Brizzolara, M. Morabito, and E. Lee, "Single- and two-phase CFD V&V for high-speed stepped planing hulls," Ocean Engineering, vol. 261, p. 112047, 2022.

[23] K. I. Matveev, "CFD simulations of basic stepped-hull configurations in calm water," Journal of Marine Science and Engineering, vol. 13, no. 7, pp. 1–24, Jul. 2025.

[24] B. P. Valtheru, "CFD analysis of resistance for stepless and stepped planing hulls," M.S. thesis, Florida Institute of Technology, Melbourne, FL, USA, 2018.

[25] ITTC, "Recommended procedures and guidelines: Practical guidelines for ship CFD applications," ITTC Quality System Manual, Rev. 05, 2024.

[26] ITTC, "Recommended procedures and guidelines: Resistance test," ITTC Quality System Manual, Rev. 05, 2021

[27] G. Budynas, Shigley's Mechanical Engineering Design, 9th ed., 2006.